33RD CONGRESS
OF THE INTERNATIONAL COUNCIL
OF THE AERONAUTICAL SCIENCES
STOCKHOLM, SWEDEN, 4-9 SEPTEMBER, 2022

ICAS 2022 SWEDEN

DESIGN AND WIND TUNNEL TESTING OF A GENERAL AVIATION BLENDED WING BODY AIRCRAFT

Franco Maurce Staub[1] & Takeshi Tsuchiya[1]

[1]The University of Tokyo, Japan

Abstract

Research over the last 3 decades has repeatedly suggested that a blended wing body (BWB) aircraft will burn about 10-30% less fuel than a tube-and-wing aircraft for the same payload and range. Despite this, we still do not see BWB aircraft in commercial service today. This study focuses on designing a BWB that is lower cost, and therefore more realizable, by reducing the scale down to a general aviation (GA) size. First, the design advantages and challenges from scaling a BWB to the GA scale are discussed. Then, two GA-scale (6-seat and 4-seat) BWBs were designed using OpenVSP and wind tunnel tested. Lessons from the first design were applied to improve the second design, which resulted in a L/D of 22.6, maximum lift coefficient of 1.156, and improved stall characteristics.

Keywords: general aviation, blended wing body, design, wind tunnel, realizable

1. Introduction

A blended wing body (BWB) aircraft is a type of aircraft, usually tailless, with its fuselage blended into the wings to improve aerodynamic efficiency for a given internal volume. Research over the last 3 decades has repeatedly suggested that a BWB aircraft will burn about 10-30% less fuel than a tube-and-wing aircraft for the same payload and range [1, 2, 3]. Despite this, we still do not see BWB aircraft in commercial service today. While there are many technical challenges that make a BWB difficult to realize, the adoption of flying wings (similar to BWBs), such as the B2 stealth bomber, for military applications proves that these challenges can be overcome.

1.1 Motivation

A less frequently discussed challenge towards realizing a BWB is that of development cost. Most of BWB literature addresses airliner-scale aircraft, which have astronomical development costs. For example, the Boeing 787 had a development cost of $32 billion [4]. If we consider the infrastructural overhaul that is necessary to manufacture a shape as different from a tube and wing (TAW) aircraft as a BWB, these costs would likely further increase. Given the limited amount of real-world experience with BWBs, there may be too many uncertainties from an investor's point of view regarding the true performance of a BWB to warrant such a large investment.

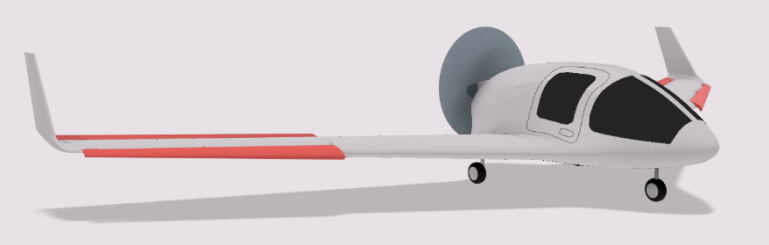

Figure 1 – Conceptual design of a 4-seat general aviation, BWB aircraft.

With that in mind, this study seeks to design a BWB that is lower cost by reducing the scale down to a general aviation (GA) size (Figure 1). The motivation is that by starting small, we can drive down the cost to make realization more palatable for investors. Having a real-world, manned BWB will 1) test the hypothesis of aerodynamic superiority purported by the literature, 2) serve as a platform to evaluate the stability (and safety), controllability, and flight handling qualities with a pilot onboard, and 3) foster investor confidence in BWB technology – given that superior aerodynamics and adequate safety can be demonstrated. This aircraft can also serve to reduce the environmental impact of GA, which is not large to begin with but is worth noting. It has been suggested in the literature that the efficiency improvements of BWBs scale with size [5]. While this may be true for airliner BWBs, which is the scope of their work, earlier studies from the 1940s and 1950s [6, 7] suggest that this trend may no extend down to propeller-driven tailless/BWB aircraft. Even at the GA-scale, the benefits of a small wetted-area-to-volume ratio can pay dividends in drag reduction. This ratio can also lead to increased internal volume for the same drag as a conventional aircraft, which has implications for low energy density fuels. This is especially relevant in light of recent developments in electric nad hydrogen aircraft at the GA scale.

1.2 Overview

In this paper, modern design tools are implemented to explore the design space of GA-scale BWBs. The unique design advantages and challenges that arise at this scale are compared against those that arise at the airliner-scale. This is done by summarizing lessons from the literature, running trade studies using NASA's OpenVSP tool in combination with MATLAB scripts [8], and applying knowledge and techniques from [9]. This knowledge is then applied to design a 6-seat, 300-horsepower piston engine, BWB aircraft in OpenVSP, use VSPAERO to evaluate its aerodynamic efficiency and stability, and validate the results in a wind tunnel. Nonlinear information related to viscous effects, control surfaces and landing gear would also be gathered in the tunnel. However, the results from this first wind tunnel experiment did not provide very promising results, and so a second aircraft was created. Lessons learned from the first wind tunnel experiment were applied to improve the performance and stability. These lessons are discussed in detail later. Additionally, the size of the second aircraft was reduced to represent a more "center-of-the-market" GA aircraft – 4 seats and a 200-horsepower engine. Again, a model was created, and wind tunnel experiments ensued. Unfortunately, the wind tunnel experienced technical problems shortly into the second wind tunnel experiment, so only the baseline configuration was tested.

The original plan was to include only the results from the improved second design, but since there is not much data available yet and the wind tunnel is still in repair, it was decided to include the results from the first design as well. After all, this design exemplifies some pitfalls when designing tailless aircraft that may be of value to readers. Lastly, there is enough overlap between the two designs to extrapolate some data from the first design onto the second, especially for control surface derivatives. The first design (6 passengers) will be called "Case 1", and the second (4 passengers) "Case 2".

2. GA-scale vs Airliner-scale BWB Design Space

2.1 Advantages

Perhaps the biggest difference between a GA aircraft, and an airliner is the power plant. From a cost perspective, a piston engine is about 1 order of magnitude less expensive than a turboprop engine, and at least 2 orders of magnitude less expensive than a jet engine. Cost aside, a piston engine will simplify the BWB design process in several ways.

Firstly, a piston engine is limited to about 5 km in altitude, however the majority of GA operations occur at 2 km or less. At these altitudes, it is no longer necessary to pressurize the cabin. For BWB airliners, cabin pressurization is known to complicate the structural design. The reason for this is that the top surface of a BWB is under compression from the wing bending moment and the cabin pressurization exerts a load orthogonal to the compression axis (Figure 2). This load case is prone to buckling, and thus great care needs to be taken when designing the centerbody upper skin (assuming an integrated structure). This challenge is not insurmountable, as evidenced by [10], but it undoubtedly complicates the design and manufacturing processes. If no cabin pressurization is required, this constraint can

be removed, simplifying and lightening the structural design. No pressurization system also reduces system complexity and allows the use of larger windows with sharper corners, which provide better pilot visibility.

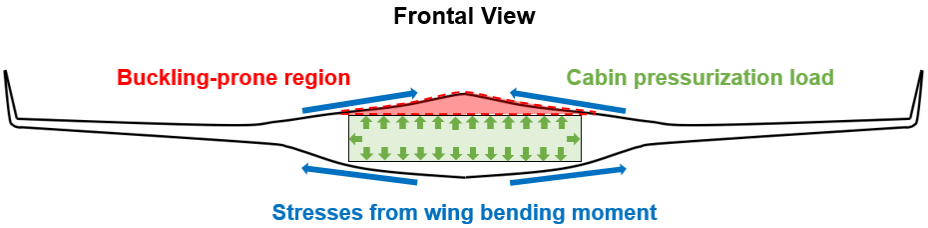

Figure 2 – Cabin pressurization loads couple with wing bending loads to create a buckling-prone region.

Another limitation imposed by a piston engine is that airspeed is limited to about Mach 0.3. For BWB airliners, the centerbody thickness ratio is constrained to about 15-17% due to the onset of compressible drag at transonic speeds [11]. This requirement is in conflict with the constraint that the cabin needs to be tall enough to fit standing people. Since GA BWBs do not fly close to transonic speeds, the thickness ratio is not constrained by compressible drag. Instead, a GA BWB will experience a pressure drag increase from a thicker centerbody, but this pressure drag behaves more predictably than wave drag, and is not as severe. Rather than using costly RANS simulations to predict transonic drag, a GA BWB's aerodynamics can be predicted with fairly good accuracy using low order solvers like VLM or potential flow methods, coupled with parasite drag build-ups. Lastly, flying slower results in smaller hinge moments. Large BWB airliners face the challenge of providing good bandwidth for an elevator that is sometimes the size of a bedroom. Hinge moments scale linearly with area and control surface chord length, and quadratically with airspeed. For a GA-scale aircraft, this problem is trivial. Also related to the controls, a GA BWBs only requires 2 to 4 primary control surfaces, making control allocation trivial.

Market	General Aviation	Regional	Single-Aisle	Twin-Aisle	Large Twin-Aisle
Size (Passengers)	4-6	120	210	300	400+
Conventional Wingspan (m)	10	35	47	61	80
BWB Wingspan (m)	12	43	64	73	80
Conventional Operable Airport (ICAO Code)	A	C	D	E	F
BWB Operable Airport (ICAO Code)	A	D	E	F	F

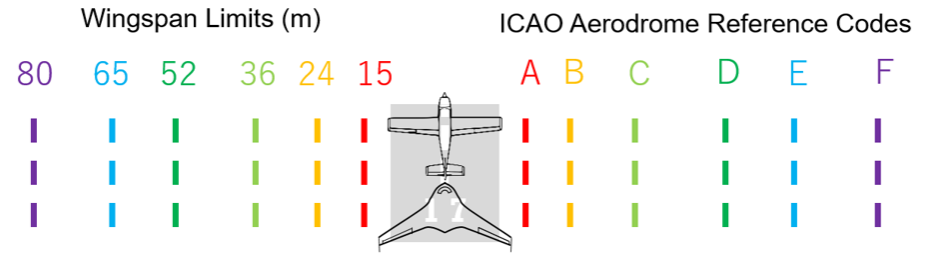

Figure 3 – Comparison of how operational constraints affect TAW vs BWB aircraft.

Another advantage for a GA BWB is that the wingspan will not violate ICAO Aerodrome Code restrictions, given that the wingspan remains under 15 meters. This is important in creating a level playing field between conventional aircraft and BWBs, since conventional aircraft wingspans tend to be sized to the upper limits of the airports in which they expect to operate. From looking at conceptual designs in the literature, BWBs generally require about 20-25% more wingspan than a TAW aircraft for the same payload. This means that in order to compete with a TAW aircraft of similar payload, a BWB needs to either reduce its wingspan and suffer the associated performance loss or be relegated to

larger airports. Piston engine GA aircraft rarely exceed 15 m. In fact, for 4-6 passenger aircraft, the wingspans tend to be around 7-12 meters, which leaves margin for a BWB to operate at the same Code A Aerodrome as competing TAW aircraft without having to compromise on performance. Figure 3 summarizes this information.

2.2 Design Challenges

Using a propeller also introduces some complications. The first is that it introduces the question of which is better, a pusher propeller or a tractor propeller. A tractor propeller has two main advantages. It receives clean, undisturbed intake air and it provides better cooling to the downstream engine during ground operations. As a tradeoff, the turbulent air in the propeller slipstream increases the drag over the body, a phenomenon known as “scrubbing”. A pusher propeller avoids this, but can face anywhere from a 2-5% efficiency decrease because its intake air is the turbulent wake of the centerbody [9]. An accurate prediction of this efficiency drop is beyond the scope of this paper. Instead, it is only considered how each propeller placement will affect the aerodynamic efficiency of the isolated airframe.

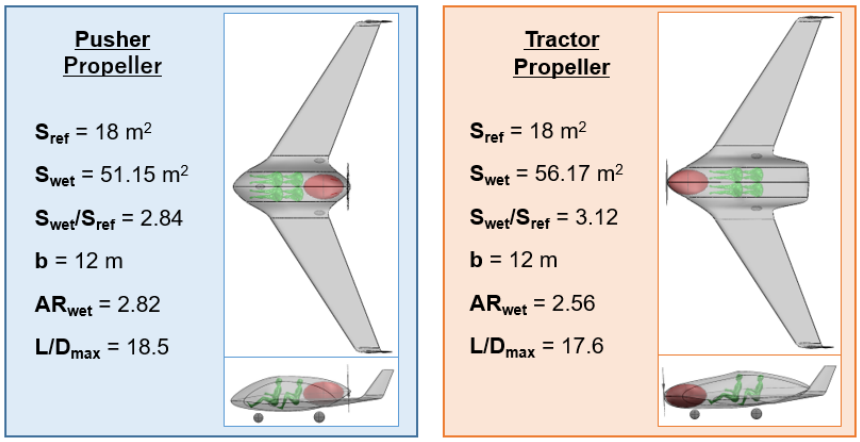

Figure 4 – Comparison of tractor vs pusher configurations.

Figure 4 shows two BWBs with the same outer wings and useful cabin space. The design features 4 passengers; and the engine, which is represented by the red ellipsoid, and is sized based on a real 200 hp engine. A pusher propeller requires that the trailing edge of the centerbody be truncated. While this increases pressure drag, it also reduces the wetted area. Meanwhile, the tractor propeller experiences a slight increase in wetted area because the nose had to be expanded to fit the engine while still providing space for 4 people. Increasing the wetted area decreases the wetted aspect ratio. Raymer [9] has shown that the wetted aspect ratio is a useful predictor of the maximum lift-to-drag ratio for a class of aircraft. When using the following relation for “retractable landing gear general aviation”:

$$\frac{L}{D}_{max} = K\sqrt{AR_{wet}} \tag{1}$$

where K = 11, it can be seen that the pusher propeller configuration has a slightly higher projected aerodynamic efficiency. This is by no means a conclusive result about the superiority of a pusher-propeller configuration. It may be possible to compensate for additional wetted area by reducing pressure and induced drag, but this is probably difficult due to the inevitably thick centerbody. Also, it remains to be seen to what extent the propulsive efficiency drops for a pusher configuration. For the rest of this paper, only pusher configurations will be discussed.

In the previous section, it was stated that there is more freedom to size the centerbody thickness since the transonic wave drag constraint does not apply. However, with this freedom comes the nontrivial decision of how thick to make the centerbody, and how far in the spanwise direction the blending area should extent. The former should be minimized to fit a given payload. To explore the latter, the pusher propeller configuration above was selected as a trade study platform (Figure 5). From it, 5

configurations with different amounts of blending were created by varying the spanwise position of the outer wing root. The further outboard it is; the more blending naturally occurs. For each amount of blending, the outer wing twist was optimized for minimum induced drag at 5° angle of attack, where the lift coefficient was roughly 0.5. The aerodynamic analysis was done using VSPAERO for the lift and induced drag, and the Schemensky 6-Series [13] form factor equation was used at 5 spanwise regions for the parasite drag estimation.

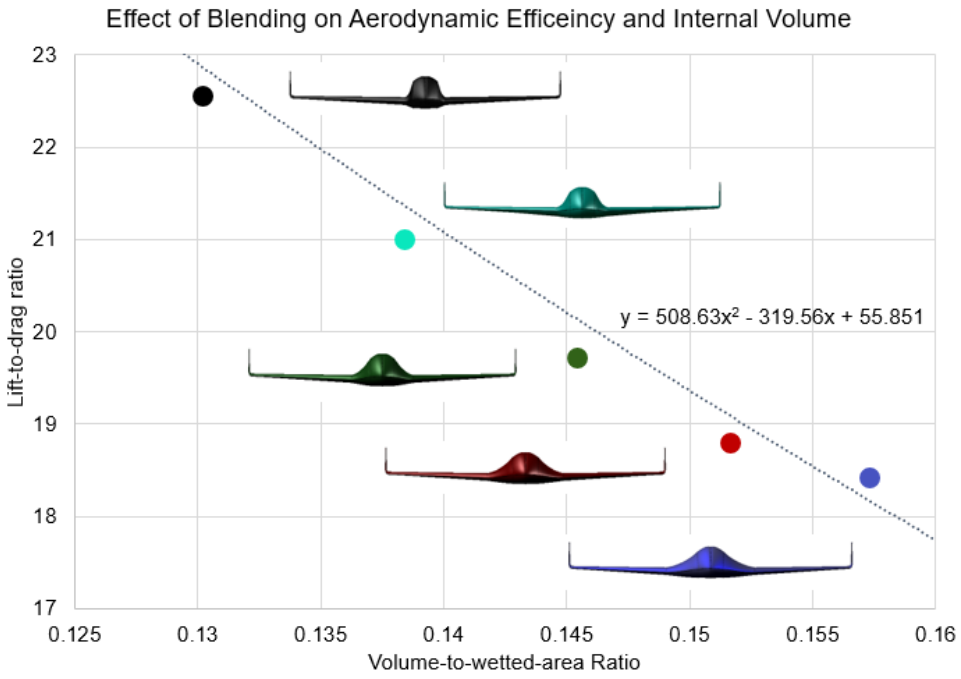

Figure 5 – Trade-off between aerodynamic efficiency and internal volume.

The results show that less frontal area yields a lower parasite and induced drag. However, if the designer were to create a more refined parameterization in the blending area, it may be possible that the induced drag could be reduced by improving the lift distribution. The current designs do not have elliptical lift distributions because the centerbody does little to produce lift. Nonetheless, it seems that parasite drag is the main determiner of aerodynamic efficiency in this design space. Even though the drag increases with blending, the resulting lift-to-drag ratios for the highly blended aircraft do not reach the levels of competing TAW aircraft (8-12 range) until large internal volumes are reached. For reference, Case 1 has a volume-to-surface-area ratio of 0.225 and an L/D_{max} of 9.7, while Case 2 has corresponding values of 0.138 and 22.6 respectively. Though these values are not plotted in Figue 5, their influence is considered in the best-fit curve. This suggests that the tradeoff between internal volume and aerodynamic efficiency is not as severe as originally thought. Low volume designs can be useful for maximizing range or speed, whereas high volume designs can still be useful for cargo, utility, or as platforms for alternative fuels with lower energy densities.

The last challenge worth noting is that BWB aircraft suffer from poor natural stability and controllability. Longitudinal stability is sensitive to center of gravity (cg) position, adverse yaw is strong, Dutch roll is poorly damped, and wingtip stall must be avoided. Airliners have the advantage of using computer augmented stability systems to address these issues. In GA, however, stability augmentation in primary flight controls has only been used for research aircraft [12], or for non-flight-critical applications like a yaw damper. The former is much too expensive for a practical GA application. The latter will almost certainly need to be adopted for adequate handling qualities. Some static stability issues will be discussed in more detail later, but a full stability analysis is beyond the scope of this paper.

3. Case 1

3.1 Design

With a general understanding of the design advantages and challenges, the next step was to create a candidate GA BWB (Figure 6). The centerbody was sized to fit 6 passengers, a 300-horsepower turbocharged engine (red box), and 300 liters of aviation gasoline. The planform was sized assuming a maximum lift coefficient of 1.0 and a stall speed of 80 knots with the max weight of 1,800 kg. Next, the wings were swept so that the static margin would range from 1% to 17% for the aft-most and fore-most centers of gravity respectively. The centers of gravity were estimated using a component-by-component mass build up in a custom spreadsheet. The wing used a NACA 65015 airfoil at the root and a NACA 65012 airfoil at the tip, and was mid-wing configuration. The winglet was made of a symmetric NACA 0010. Only 2° of washout were applied in order to create a zero pitching moment at the aerodynamic center. As will be discussed later, many of these design decisions were poorly informed.

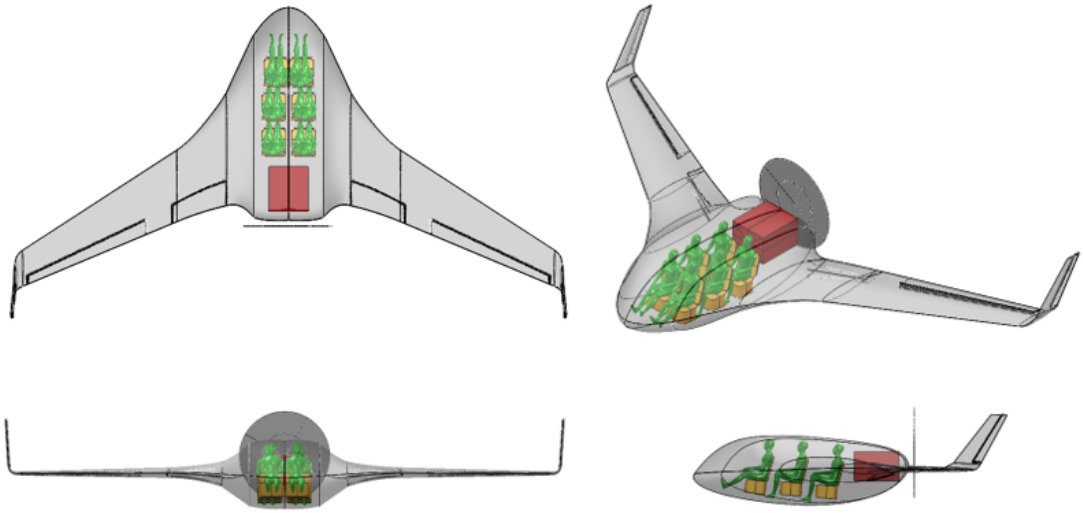

Figure 6 – Case 1: 6-seat, 300 hp engine BWB.

Initial aerodynamic evaluations varied considerably depending on which parasite drag calculation method, specifically which form factor equation, was used. At the time of designing Case 1, it was still unknown which form factor equation gave the most accurate results. Due to the very large thickness ratio of the centerbody, each equation yielded largely different parasite drag values. This is because form factor equations are typically high-order polynomial functions of thickness ratio. As a first guess, Raymer's method was used, leading to a parasite drag of 143 counts. By combining this value with the VSPAERO results for the induced drag and lift, the maximum lift-to-drag ratio was 19, which was considered optimistic. Thus, in order to get a more reliable drag prediction, a wind tunnel model was built.

3.2 Model Manufacturing

The wind tunnel model was created as follows. First, a step file of the aircraft was exported from OpenVSP to Fusion 360, where the model details for modularity and assembly were designed. Th 7.4% scale led to a model wingspan of 85 cm. The elevons were designed to be interchangeable with other elevons of various deflections by using two M2 bolts. The winglet rudders and flaps were 3D printed as triangular wedges (Figure 7). The model also featured 3 nuts glued into the lower centerbody surface so that landing gear could be screwed on. Lastly, a motor mount was built in the rear, with an internal wiring slot that fed into the hollow centerbody, where a battery and ESC could be placed. This was done with the goal of testing the aero-propulsive effects of the propeller on the centerbody, but was never used. The major centerbody components were bonded together using glue. After this, a layer of epoxy was added over the surface and sanded to an acceptably smooth finish. Lastly, 2 layers of primer where sprayed on top.

The University of Tokyo Hongo Low Speed Wind Tunnel was built in 1940, and thus features very old technology. The model is fixed with tensioned wires that attach to load cells. The positioning of the load cells is fixed, and therefore determines the attachment points to the aircraft. Two wires attach on each leading edge at approximately the half-span location, and another wire attaches 45 cm behind this at the center. Since this aircraft has no tail, an extension jig had to be attached to reach this last wire. The load cell analog signals are converted to digital, and recorded on a Linux PC using a script that averages samples over about 5 seconds. An image of the CAD model, and the real model in the tunnel is shown in Figure 7.

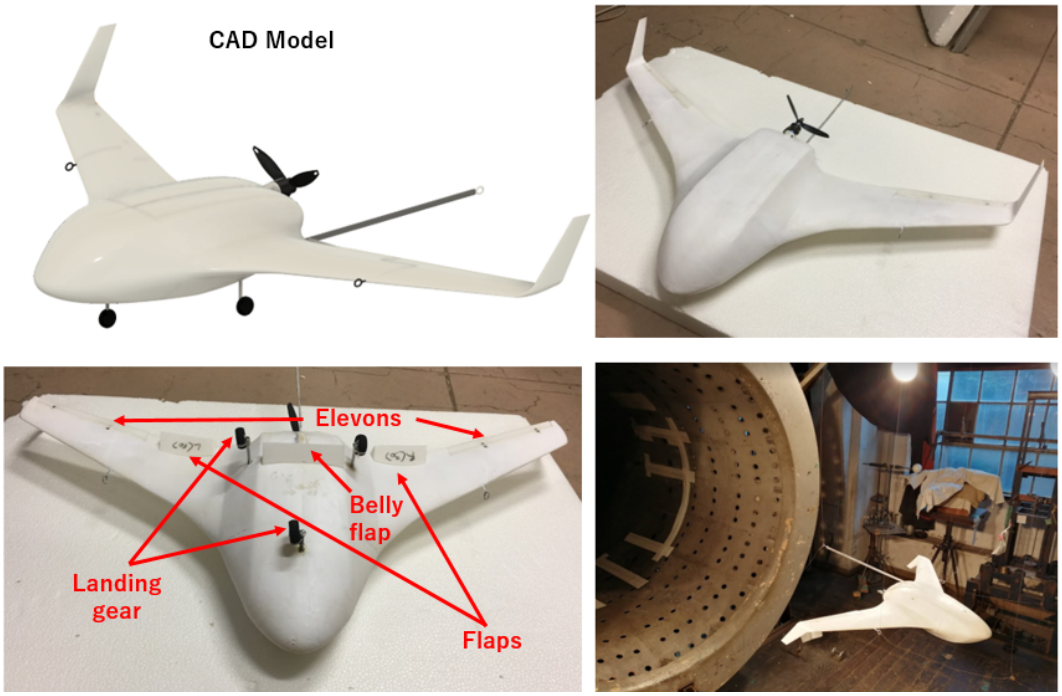

Figure 7 – Upper left: CAD image of Case 1 wind tunnel model. Rest: real model with details and wind tunnel set up.

3.3 Wind Tunnel Test Procedure

The wind tunnel has the capability of measuring lift, drag, pitching, rolling, and yawing moments. For Case 1, angle of attack was adjustable from -14° to 16°, and all cases were run at 20 m/s airspeed. The corresponding Reynolds number was 2.5 x 10^5. Nonzero sideslip angle measurements and side force measurements were not possible for this experiment. Separate “jig only” runs were conducted to account for its aerodynamic effects, however it was ultimately not possible to capture reliable data. As a result, the jig drag contribution was estimated using the OpenVSP Parasite Drag module. The wire drag was calculated from the total wire frontal area, the dynamic pressure, and a drag coefficient of 0.8.

The procedure was the same for all configurations, except more data points were taken for the clean baseline configuration. In addition to this clean baseline configuration, a 10° aileron deflection, 10° elevator deflection, 30° rudder deflection, 60° rudder deflection, 30° flap deflection, and a landing gear configuration were also tested. Other novel control surfaces, such as a “belly flap” and a “stall shield”, were also tested. For brevity, these results will be omitted.

3.4 Results

Figure 8 shows the results for the longitudinal aerodynamics and compares them with the equivalent VSPAERO results. The baseline configuration shows a very low C_{Lmax} of 0.676, lots of drag, and a wingtip stall at 6° angle of attack. The low C_{Lmax} is due to the large, thick centerbody area. A large centerbody is beneficial for C_{Lmax} so long as it behaves as a wing. For large BWBs, the centerbody thickness ratio is much smaller, so it behaves as wing. In this case, however, the centerbody has

thickness ratios between 30% and 40%, so it behaves more like a fuselage – a very wide fuselage that consumes large amounts of outer wing area. Unfortunately, this C_{Lmax} is further exacerbated by trim requirements. For positive static margins, an upward elevon deflection is required, which slightly reduces the C_{Lmax}. One effective countermeasure to these lift reductions is to add inboard trailing edge flaps. 30° of these flaps brought the C_{Lmax} up to 0.88, for a small pitching-moment, but large drag penalty. The flaps nearly doubled the total drag, which was large to begin with. The large minimum drag (292 counts) is also attributed to the pressure drag from the large centerbody form factor and the sharply truncated aft centerbody. This led to a small maximum L/D of 9.7.

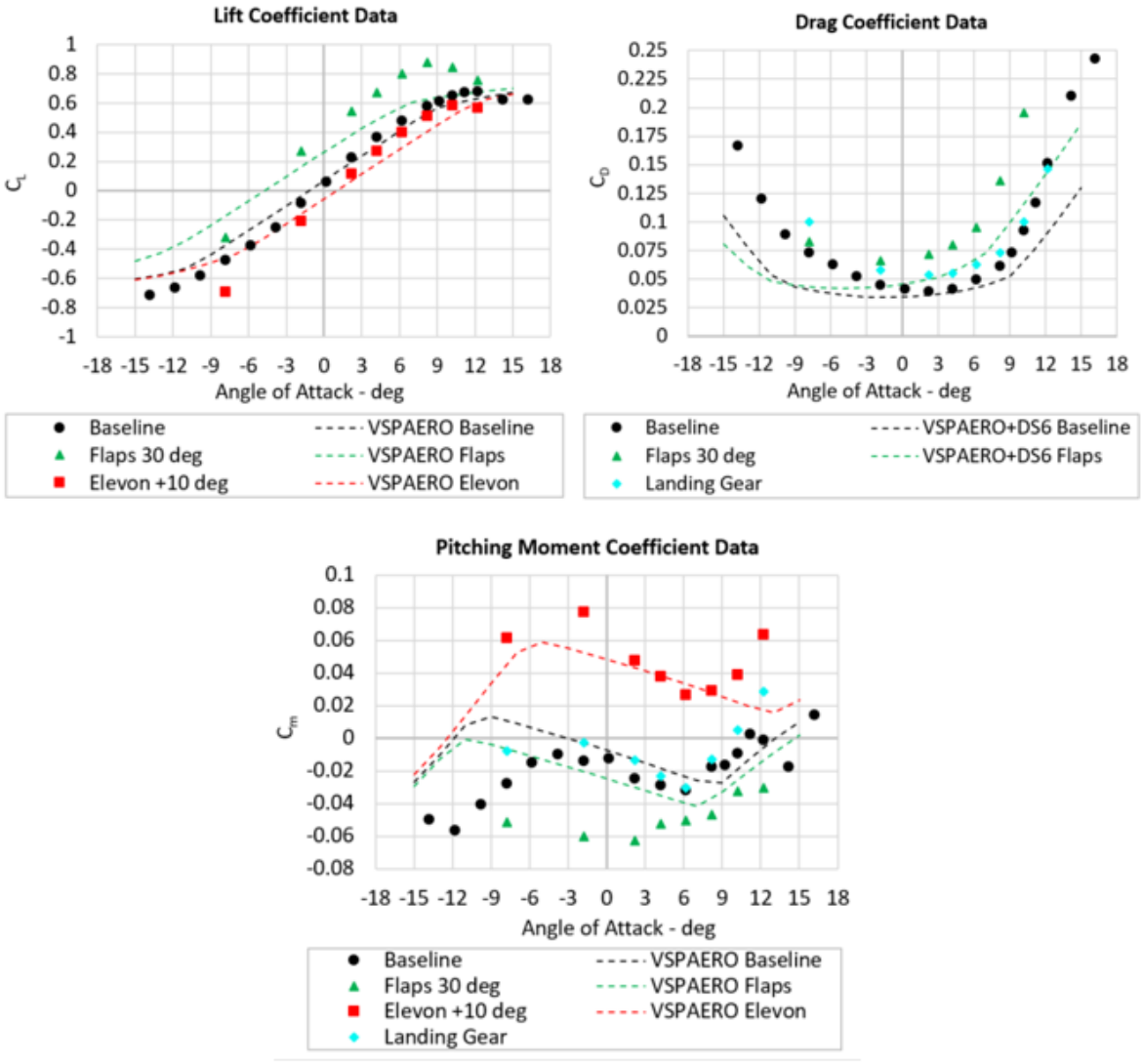

Figure 8 – Longitudinal aerodynamics: wind tunnel vs VSPAERO

Perhaps the most important issue uncovered from the wind tunnel experiment was that of pitch instability. This design serves as a great example of the consequences of not using enough washout; only 2° were used. The slope increase at 6° in the $C_m - \alpha$ curve indicates the occurrence of wingtip stall. This is followed by a momentary stability recovery between 11° and 14°, but then another larger instability starting at 14°. The recovery is likely due to the wing root stalling, however the source of the last instability is unknown. Perhaps, this is the point where the centerbody experiences significant flow separation over the top surface. Since drag plays an increasingly important role in pitching moment as angle of attack increases, the drag forward of the aerodynamic center (due to centerbody flow separation) is larger than the drag behind the aerodynamic center (due to outer wing flow separation). The result would be a destabilizing pitching moment. The important takeaway is that linear approximations of $C_m - \alpha$ apply only for a very small region of angles of attack – in this case an even smaller range than for the $C_L - \alpha$ relations. This is especially relevant when working with inviscid CFD

solvers to find trimmed flight conditions.
As stated earlier, VSPAERO was used to evaluate the aircraft, however during the design stage, no C_{Lmax} correction was used. Hence, poor stall characteristics were not uncovered until after the wind tunnel experiments. The curves in the Figure 8 use a local, 2D C_{lmax} correction to account for flow separation. When using a conservative value of 0.8, corresponding to the maximum lift coefficient for the wing airfoil at the lowest local Reynolds number, fairly accurate stall predictions were captured. C_{Lmax} and C_m nonlinearities for the clean configuration were fairly accurate, and the drag rise due to stall was also captured. Drag was again calculated by combining the VSPAERO induced drag with the parasite drag calculated using the "distributed Schemensky 6-series" described before and is marked with "VSPAERO+DS6" in the plots. The drag was slightly under-predicted and does not capture the asymmetry about the zero lift angle. It does, however, partially capture the left- and upward shift of the lift and drag curves with inboard flaps.
The results for the cases with elevon and flap deflections showed correct trends, but the absolute values were less accurate than they were for the baseline configurations. The flap C_{Lmax} increase was not captured due to the conservative, 2D C_{lmax} lift suppression. In reality, the inboard C_{lmax}, where the flaps are located, is likely higher than 0.8. This method also produced optimistic wingtip stall angles for the elevon-up configuration. While the indicated elevon deflection does decrease the wingtip local C_L, it also changes the pressure distribution substantially from the airfoil that was used to predict the C_{lmax}. Hence, the real stall pattern differs from the VSPAERO prediction.

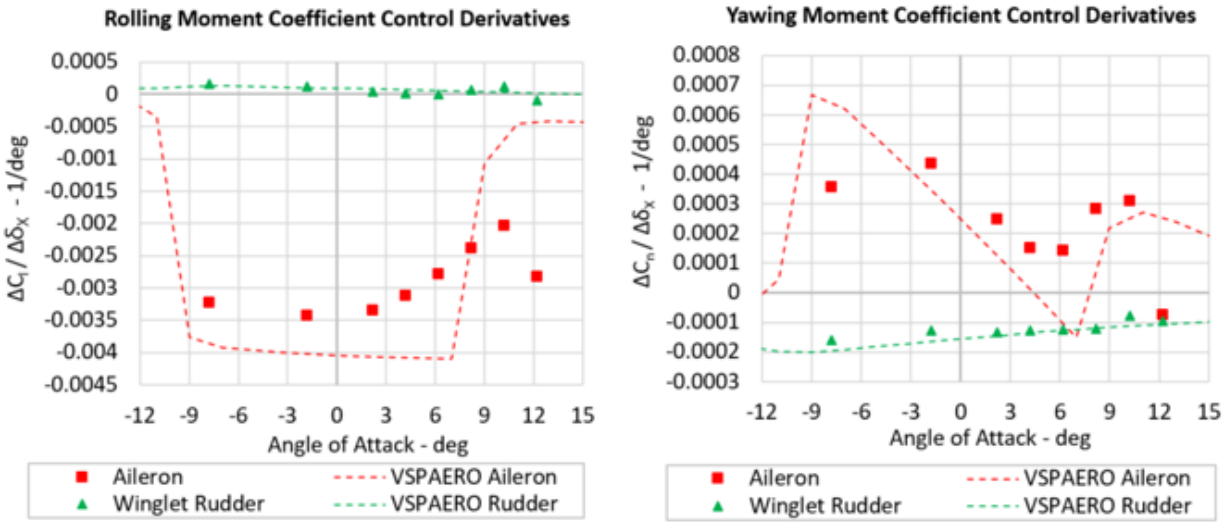

Figure 9 – Roll and yaw moment control derivatives: wind tunnel vs VSPAERO

While the current wind tunnel setup did not allow for sideslip measurement, it did provide some insight into some of the lateral-directional control derivatives. This data is shown in Figure 9. The positive roll direction points out the back of the aircraft, and the positive yaw direction points out the top of the aircraft. From looking at the aileron data, it can be seen that roll authority is decreased at higher angles of attack. Also, the bump in the yawing moment from 6° to 10° suggests that the wing with the downward elevon deflection stalls first, producing a momentary increase in adverse yaw. The rudder data is fairly constant, with a slight reduction in yaw effectiveness at high angles of attack. The rudder authority per degree of deflection is also clearly much lower than the adverse yaw per degree of aileron deflection. This is compensated by having a large rudder deflection range – up to about 60° as compared to 20° for ailerons. The wind tunnel data suggested that the rudder yawing moment is linear with respect to deflection angle until at least 60°, unlike other differential-drag-based yaw control devices (i.e. split rudders).
VSPAERO again provided fairly accurate results – especially in the case of the winglet rudder. The aileron rolling moment was over-predicted and the nonlinearities, such as the wingtip stall adverse yaw and aileron loss of effectiveness, are exaggerated. VSPAERO suggests there is a proverse yaw from 4° to 8°. This is probably because the drag is under-predicted in this range. Since the lift vector

points forward in the body frame at high angles of attack, it would generate a proverse yaw if the drag is sufficiently small. This effect exists in the wind tunnel data, but not to the extent that proverse yaw is generated. VSPAERO results also suggest there is a sharp drop-off in aileron roll authority at the stall angle, while the wind tunnel data show this authority loss is more gradual.

3.5 Lessons Learned

From both aerodynamic efficiency and stability standpoints, Case 1 was clearly a failed design. The only upside was the comparatively large internal volume. With failed designs, however, come valuable lessons, which will be summarized in this section.

3.5.1 Lesson 1: Working in the design space between a wing and a fuselage

In regards to aerodynamic efficiency, the problem for this design was most likely the oversized centerbody. Unless the aft centerbody is stretched into an airfoil shape – which would reduce the thickness ratio – the centerbody should not be expected to produce any significant lift. The corollary is that any projected wing area that sits inside the centerbody is effectively nonexistent like in the case of a TAW aircraft, except since the centerbody is exceptionally wider than TAW fuselages, more wing area is lost. As a first lesson and a rule of thumb: "wing sections" with thickness ratios greater than 25% that do not have a sharp trailing edge do no produce significant lift. Hopefully, this can serve as a quantitative reference for those designing something in between a wing and fuselage.

3.5.2 Lesson 2: Understanding the details behind analysis tools being used

At the time of creating Case 1 in OpenVSP, it was not realized that the Parasite Drag module calculates form factors based on the global maximum thickness ratio. This method fails to account for spanwise variability in thickness ratios, which is fine for most applications since most wings have thicknesses well under 20% along the full span. However, in Case 1 the thickness varies from 10% at the tip to 40% at the blending section, so using a form factor corresponding to 40% thickness ratio will lead to an overestimation, especially if most of the span consists of thinner wing sections. To illustrate this point, according to the current version of OpenVSP's (3.27) Parasite Drag tool, the two wings in Figure 10 have the same amount of parasite drag.

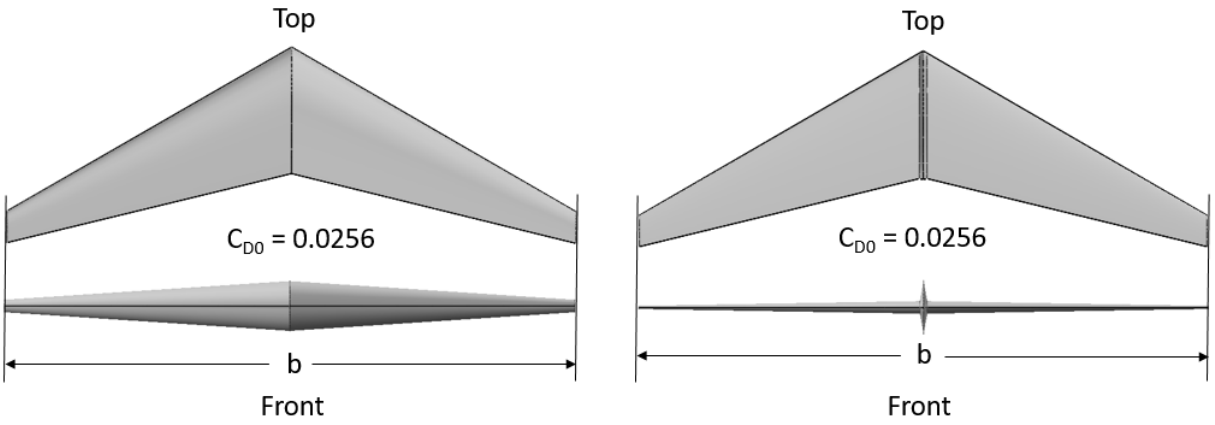

Figure 10 – Parasite drag estimates for two wings of identical flow conditions and planforms, but different thickness distributions using OpenVSP Parasite Drag module

Now, depending on which form factor equation is used, very optimistic drag predictions can still be ascertained for thick wings. These two points led to the parasite drag – clearly a very important factor in this design – to be difficult to predict with confidence. It was only after gathering wind tunnel data and trying several manual approaches that it was decided that the Schemensky 6-Series AF method, when applied to each spanwise section individually, provides reasonable estimates. Hence, this method was used for all parasite drag calculations in this paper. Also, note that since this feature is not built into OpenVSP's Parasite Drag module, it must be done manually or with a script. In summary, the second lesson is to understand what is happening under the hood of the aerodynamic

tools being used. This revealed that pressure drag, more so than induced or skin friction drag, was responsible for the large total drag. When pursuing drag reduction for Case 2, this information was of central importance.

3.5.3 Lesson 3: Aerodynamic center of a BWB moves more than for a TAW aircraft

It is well-known that aerodynamic center positions move, but often overlooked that this movement is more pronounced in tailless aircraft. There seem to be many BWB papers that assume stationary aerodynamic centers. This is fine for low angle of attack analysis, but even then, Case 1 shows how early wing stall can develop. Therefore, it is worth reiterating the importance of this point for future designers.

Textbooks often describe the aerodynamic center as a fixed point where the pitching moment does not change with respect to lift coefficient. To reinforce this oversimplification, inviscid solvers (without C_{Lmax} limiters), provide linear $C_m - \alpha$ curves. In principle, horizontal stabilizers add enough stability to an aircraft so that that this assumption works. However, when there is no horizontal stabilizer to dampen out wing instabilities, every flow change on the wing is felt at the aerodynamic center. Most importantly, extreme care needs to be taken to design a wing with a safe stall pattern: namely a root stall. Hindsight reveals that even though stalling is a viscous effect, meaning it is difficult to predict without viscous solvers (i.e. RANS, LES), there are effective tools for first-order approximations. When used conservatively, they can prove to be useful for C_{Lmax} estimation, and to a lesser extent, $C_m - \alpha$ curves. Additional guides for preventing wingtip stall can be found in [14, 15, 16], which contain wind tunnel data on a variety of wing planforms. [14] can also be used as a first-order predictor of wingtip stall behavior based on the sweep angle and aspect ratio alone. Note that the wings used to develop this prediction method were not washed out, meaning there is some margin to recover a “wingtip stall” wing to a “root stall” wing with washout. Unfortunately, all these sources were only uncovered after the wind tunnel test, and so their wisdom was overlooked. The design for Case 1 had only 2° of washout, a fairly high aspect ratio (7.2) and high sweep (33°). This combination led to very early wing tip stall at a C_L of only 0.5. Since it is impossible to manually control the pitch beyond this angle, the effective C_{Lmax} is also reduced to this value. From all this, the third lesson is to design for root stall as much as possible at the first design stage. It will save a lot of high-lift device or flow separation “patch work” down the road. Achieving good stall behavior is at least as important as getting the correct static margins: they are both of central importance.

3.5.4 Lesson 4: Zero moment at the design lift coefficient and nominal static margin

In the "Design" section, it was stated the wing was washed out to create zero pitching moment at the aerodynamic center with no elevon deflection. This statement is equivalent to saying that there will be no pitching moment for a static margin of 0 or, in other words, that the $C_m - \alpha$ curve at zero static margin is both null in absolute value and slope. In reality though, the static margin will not be 0; it will be some positive (assuming natural stability) value (1%-17% for Case 1). This means that even for the aft-most cg, there will be trim drag, and at the forward cg, the trim drag will be large and consume significant amounts of elevator bandwidth. A better solution is to select one or several design lift coefficients, determine the nominal static margin – corresponding to a cg in between the forward and aft positions – and wash out the wing until the pitching moment is zero at these conditions. This will lead to some tail-heaviness (positive pitching moment) at below-nominal static margins and low angles of attack, but it will reduce the trim drag across the operating envelope, and lead to more pitch-up elevator bandwidth at high angles of attack. This is lesson 4: to consider a *nonzero, nominal* static margin when washing out the wing to achieve zero pitching moment at the desired lift coefficient(s).

As a final note regarding these lessons: these are not necessarily new, nor are they a comprehensive rule set for designing a GA BWB. The reader is referred to books such as [17] or papers like [1, 2, 14, 15, 16] for further guidance. The lessons above are just the ones are exemplified well by Case 1, and are considered issues that do not seem to be stressed enough in many modern BWB/tailless aircraft design papers.

4. Case 2

The design process for Case 2 was informed based on the lessons learned from Case 1. The main motivations were to reduce the centerbody thickness ratio and width, produce a zero pitching moment at a nominal static margin, and reduce the severity of the wingtip stall problem. Additionally, the size was reduced from a 6-seat to a 4-seat aircraft. This decision was unrelated to the motivation to reduce the centerbody. Rather, it was decided that a 4-seat, 200 hp piston engine aircraft is a more standard size for the GA market. The number of seats is not expected to have a significant effect on the achievable aerodynamic efficiency.

4.1 Design

Several details of the design process are the same as for Case 1. First the wing was sized based on stall requirements, then the cabin was manually designed to seat 4 people and a typical 200 hp engine. Finally, the outer wing sweep was determined by static margin constraints, and then washout was applied in order to trim out pitching moment.

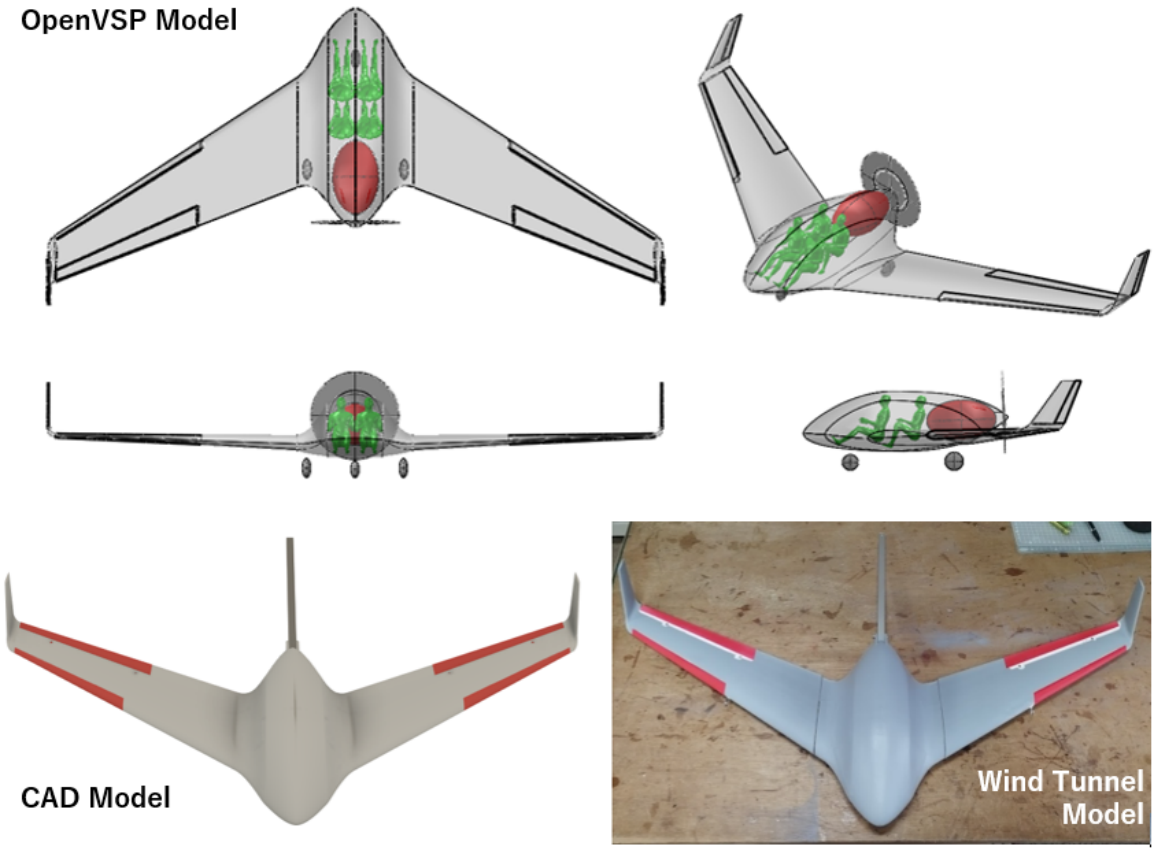

Figure 11 – Case 2: 4-seat, 200 hp engine BWB. OpenVSP model, CAD model, and wind tunnel model are shown.

Due to the low C_{Lmax} from the wind tunnel, the C_{Lmax} used for the wing sizing was reduced from 1.0 to 0.8. From real world aircraft, the maximum takeoff weight for a 4-seat, GA aircraft with a 200 hp engine is about 1,400 kg. Using a stall speed of 80 knots led to a wing size of 18 m^2. The centerbody was again designed manually. This time, very little space was left between the internal components and the outer skin. Thus, the internal volume was reduced significantly. The engine was modeled as an ellipsoid with dimensions taken from a Continental IO-360 engine, and the trailing edge of the centerbody was tapered to tightly envelop this ellipsoid volume, leading to a more streamlined aft centerbody. The sweep angle was again decided by the constraint of having a positive static margin for the aft-most cg position, which was 33°. The outer wing airfoils were changed from the cambered NACA 6-series to zero-moment, reflexed MH-60 airfoils. The thickness of the airfoil was increased to 14% at the wing root, and 12% at the wing tip. Like in Case 1, the washout was determined by

minimizing the induced drag for the cruise CL, except this time, the static margin was set to 8%. The resulting washout was 5°.
This washout was more reasonable from a wingtip stall perspective, but it still produced a rear-up stall when evaluated with VSPAERO. Unfortunately, this rear-up stall persisted in VSPAERO, even with very large amounts of washout. From this, two hypotheses were made: 1, the amount of washout necessary to entirely eliminate the rear-up stall behavior would create so much induced drag that the aerodynamics of the configuration would be compromised, and 2, that some sort of additional aerodynamic device would be necessary to generate a more desirable stall response. In this case, outboard slats were chosen as one approach. These were designed by hand using the data from [18] as a reference. Additionally, inboard flow tripping devices such as spoilers and stall strips would also be evaluated. However, these have not been tested yet. The resulting design is shown in Figure 11. Images of the CAD model and wind tunnel model are also shown.

4.2 Results

As mentioned in the Overview section, due to technical issues with the wind tunnel, it was not possible to gather the full aerodynamic data set for this configuration in time. Only data for the baseline configuration was gathered. This is shown in Figure 12.

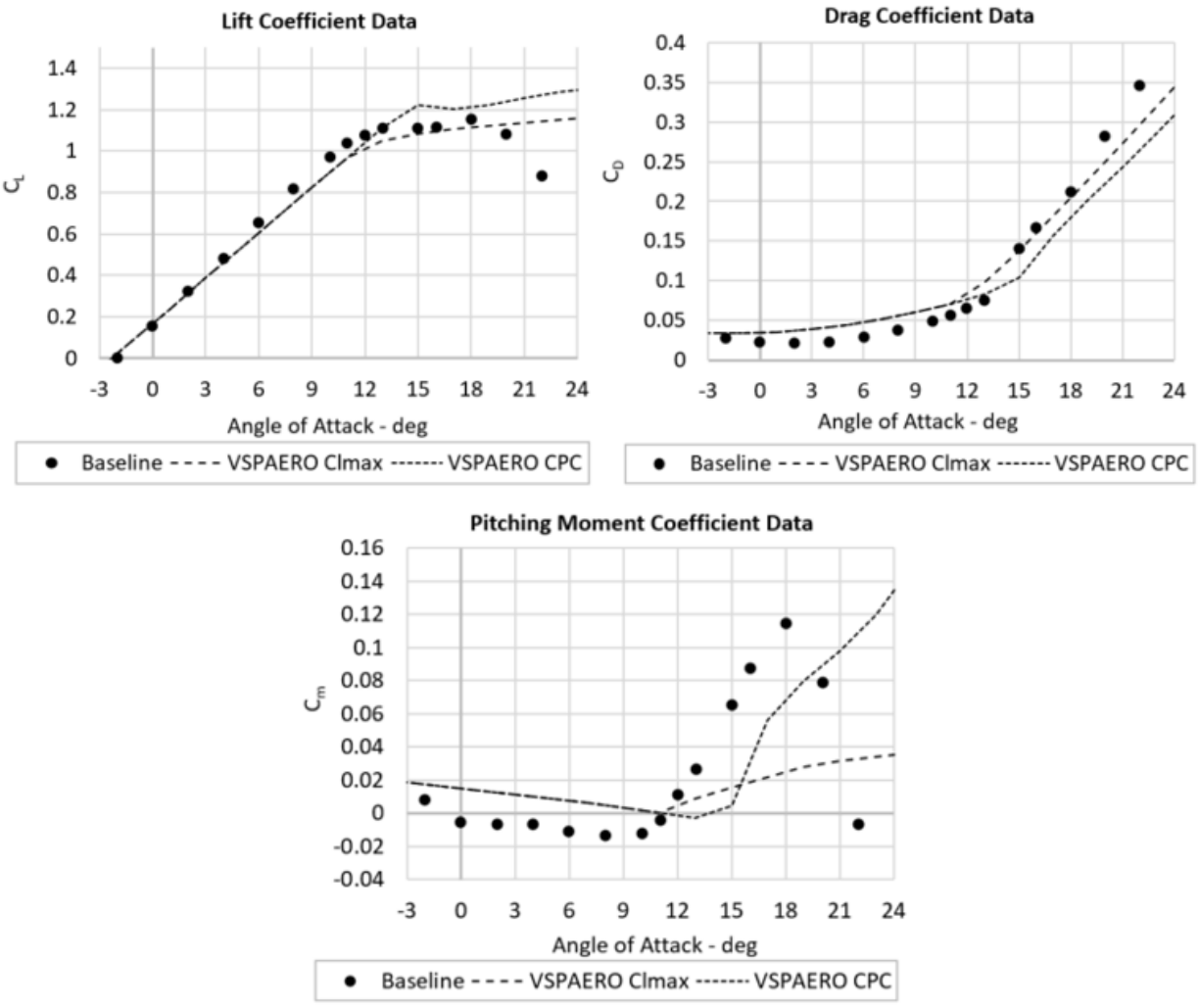

Figure 12 – Longitudinal aerodynamics: wind tunnel vs VSPAERO

Case 2 exhibits marked improvements over Case 1. The C_{Lmax} increased to 1.156, the minimum drag reduced to 211 counts, and pitch instability was shifted to a higher angle of attack, extending the stable-pitch region. The C_{Lmax} increase is mainly the result of two factors, using an airfoil with a higher C_{Lmax}, and increasing the exposed wing area, which is a result of a larger total planform and smaller centerbody. The drag reduction is attributed to a lower thickness ratio for the centerbody section.

Compared to the maximum thickness ratio of 40% in Case 1, Case 2 had only 31% thickness at the blending area. Additionally, the tapering of the aft centerbody was much more gradual as can be seen by comparing Figures 6 and 11. This likely further reduced the pressure drag. The reduced drag created a maxinmm lift-to-drag ratio of 22.6. The shift of the stall angle was also due to two factors. First, the MH-60 has a higher stall angle than the NACA-63015. Second, the washout was more than double that of Case 1. Where Case 1 experienced a gradual stall starting from the wingtip and moving inboard, Case 2 seemed to experience a full-wing stall simultaneously. This was observed by sweeping a tuft on a rod across the span at each angle of attack and taking notes on the flow pattern. While a simultaneous, full-wing stall is undesirable, the data suggests that beyond this stall, there is a sharp nose-down moment to prevent the aircraft from entering a pitch tumble. This type of stall behavior has been well documented in by flying wing pilots in [17]. Lastly, since the clean wing stalls all at once, it is expected that an outboard slat will delay the wingtip stall just enough to result in a root stall. If this is indeed the case, the benefits of a docile stall at low speeds can be attained without compromising the low drag at high speeds. Of course, this remains to be confirmed.

As in Case 1, VSPAERO results were fairly accurate for the Baseline configuration. For comparison, two C_{Lmax} models are included. The data labeled "Clmax" uses 2D airfoil data for the outboard wing section and the corresponding Reynolds number as described before. The resultant C_{lmax} used was 1.0. The "CPC" method refers to the Carlson Pressure Correlation built into VSPAERO [19]. While the Clmax method provided more accurate stall angle and C_{Lmax} predictions, the CPC method more accurately predicted the severity of the pitch up moment. It is the author's understanding that this method was developed with the main goal of predicting where stalling begins, rather than the aerodynamic forces and moments post-stall. Thus, more accurately predicting the $C_m - \alpha$ curve slope may be irrelevant. Overall, the Clmax method provides a more conservative estimate. This may be more suitable since the Reynolds number (2.5 x 10^5) for this experiment is on the lower end of what the CPC method seems to have been developed to accurately predict. In either case, VSPAERO provides very satisfactory results considering the model simplicity and fast calculation times.

5. Conclusion

In this paper, the design and wind tunnel testing of a GA BWB were presented. First, the motivations behind designing a BWB at this small scale were discussed. A GA BWB is many orders of magnitude less expensive than an airliner-scale BWB; and if aerodynamic efficiency and adequate stability can be demonstrated, it can directly improve the state of GA, while also serving as a data point to incentivize the pursuit of larger BWBs.

GA BWBs have some unique advantages and challenges in comparison to large BWBs. While the challenges and advantages for large scale BWBs are well-known, there is not much literature discussing the design space of GA-scale BWBs. In summary, GA BWBs face fewer structural limitations, can be created with a thicker centerbody and can fly in the same airspaces as similar-sized TAW aircraft, but they face the challenge of propeller integration, a lack of options when it comes to stability augmentation systems, and poor lift generation at the centerbody, which makes achieving elliptical lift distributions difficult. Initial trade studies suggest that the spanwise thickness ratio distribution plays a major role in the aerodynamic efficiency vs internal volume trade-off.

To evaluate the aerodynamic efficiency and stability of a GA BWB, a 6-seat, 300 hp engine BWB called "Case 1" was design in OpenVSP, and tested at 7.4% scale in a wind tunnel. The results were poor, showing a low L/D_{max} of 9.7, and wingtip stall at a low C_L of 0.5. Many lessons were learned from this design, the most important of which are summarized as follow. The boundary between a wing and a fuselage becomes unclear at high thickness ratios (>25%). It is best assumed that these sections produce negligible lift. Parasite drag predictions can vary significantly with thick sections because form factors are usually higher-order polynomial functions of thickness ratio. Also, wingtip stall needs to be a central consideration in the first stage of BWB design. Lastly, the aerodynamic shape should be designed around operating points at nominal static margins, not about the aerodynamic center.

Using these lessons, a second BWB, Case 2, was designed. In this case the size was reduced to 4 seats and a 200 hp engine because this is a more "center-of-the-market" GA aircraft. The data for the baseline configuration showed dramatic improvements over Case 1. The drag was 28% lower, the C_{Lmax} was 71% higher, and the stall behavior improved. Rather than a wingtip stall well below

the C_{Lmax}, a full-wing stall occurred very near the C_{Lmax}. The lift-to-drag ratio for Case 2 was 22.6, as compared to 9.7 for Case 1. These results suggest that a BWB with superior aerodynamic efficiency can be designed even at the small, GA scale.
Due to technical issues with the wind tunnel, only the baseline configuration for Case 2 was tested. Once the tunnel is fixed, additional configurations including control surface deflections, extended outboard slats, and root-stall devices will be tested for Case 2. These results, a full stability analysis, piloted simulations, and performance calculations are all topics that will be considered in future work.

6. Contact Author Email Address

Franco Staub - PhD Candidate
The University of Tokyo
francostaub@g.ecc.u-tokyo.ac.jp

7. Copyright Statement

References

[1] Liebeck R. Design of the Blended Wing Body Subsonic Transport. *AIAA Journal of Aircraft*, Vol. 41, No. 1, Jan-Feb 2004.

[2] Page M, Smetak E and Yang S. Single-Aisle Airliner Disruption with a Single-Deck Blended-Wing-Body. *31st Congress of the International Council of the Aeronautical Sciences*, Belo Horizonte, Brazil, 2001.

[3] Nickol C and Haller W. Assessment of the Performance Potential of Advanced Subsonic Transport Concepts for NASA's Environmentally Responsible Aviation Project. *SciTech Forum: 54th AIAA Aerospace Sciences Meeting*, San Diego, CA, USA, 2016.

[4] Nolte P, Gollnick V. Definition and Selection of Air Transportation System Requirements based on "a posteriori" knowledge. *12th AIAA Aviation Technology, Integration, and Operations (ATIO) Conference and 14th AIAA/ISSM Multidisciplinary Analysis and Optimization Conference*, Indianapolis, IN, USA, Sep 2012.

[5] Reist T, Zingg D. Optimization of the Aerodynamic Performance of Regional and Wide-Body-Class Blended Wing-Body Aircraft. *33rd AIAA Applied Aerodynamics Conference*, Dallas, TX, USA, Jun 2015.

[6] Northrop J. The Development of All-wing Aircraft. *The Aeronautical Journal: 35th Wilbur Wright Memorial Lecture at The Royal Aeronautical Society*, Volume 51, Issue 438, pp. 481-510, June 1947.

[7] Lee G. The Case for the Tailless Aircraft. *The Royal Aeronautical Society*, Volume 50, Issue 431, pp. 872-887, November 1946.

[8] Kim J, Tsuchiya T. OpenVSP Based Aerodynamic Design Optimization Toll Building Method and Its Application to Tailless UAV. *33rd Congress of the International Council of the Aeronautical Science*, Stockholm, Sweden, Sep 2022.

[9] Raymer D. *Aircraft Design: A Conceptual Approach*. 5th edition, AIAA Education Series, 2012.

[10] Jegley D and Velicky A. Development of the PRSEUS Multi-Bay Pressure Box for a Hybrid Wing Body Vehicle. *56th AIAA Applied Aerodynamics Conference: SciTech 2015*, Kissimmee, FL, USA, 2015, Session: Design, Test and Analysis II, AIAA 2015-3292.

[11] Bradley K. A Sizing Methodology for the Conceptual Design of Blended-Wing-Body Transports. *NASA Contractor Report; George Washington University, Joint Institute for the Advancement of Flight Sciences*, NASA/CR-2004-213016, Langley Research Center, Hampton, VA, USA 2004.

[12] Falkena W. *Investigation of Practical Flight Control Systems for Small Aircraft*. Doctoral Thesis, Technical University Delft, 2012.

[13] Schemensky, R. *Development of an Empirically Based Computer Program to Predict the Aerodynamic Characteristics of Aircraft*. Springfield: National Technical Information Service, 1973.

[14] Shortal J, amd Maggin B. *Effect of Sweepback and Aspect Ratio on Longitudinal Stability Characteristics of Wings at Low Speeds*. Technical Note No. 1093. National Advisory Committee for Aeronautics, Langley Memorial Aeronautical Laboratory, Langley Field. VA, USA 1946.

[15] Seacord C, Ankenbruck H. *Effect of Wing Modifications on the Longitudinal Stability of a Tailless All-wing Airplane Model*. Advance Confidential Report L5G23. National Advisory Committee for Aeronautics, Langley Memorial Aeronautical Laboratory, Langley Field. VA, USA 1945.

[16] Soule H. *Influence of Large Amounts of Wing Sweep on Stability and Control Problems of Aircraft*. Technical Note No. 1088. National Advisory Committee for Aeronautics, Langley Memorial Aeronautical Laboratory, Langley Field. VA, USA 1946.

[17] Nickel K and Wohlfahrt M. *Tailless Aircraft in Theory Practice*. 1st edition, Butterworth-Heinemann, and imprint of Elsevier Science, 1994.

[18] Schuldenfrei M. *Wind Tunnel Investigation of an NACA 23012 Airfoil with a Hangley Page Slat and Two Flap Arrangements*. Advance Restricted Report. National Advisory Committee for Aeronautics, Langley Memorial Aeronautical Laboratory, Langley Field. VA, USA 1942.

[19] Carlson H, Walkley K. An Aerodynamic Analysis Computer Program and Design Notes for Low Speed Wing Flap Systems. *NASA Contractor Report 3675; Kentron International Inc.*, NAS1-16000, Langley Research Center, Hampton, VA, USA 1983.